Static dielectric response of charged bosons

G. Sugiyama, C. Bowen,* and B. J. Alder*
Lawrence Livermore National Laboratory, Livermore, California 94550
(Received 26 May 1992)

The dielectric function of a charged Bose gas is determined from the response to an imposed static sinusoidal electric field. Variational and diffusion quantum Monte Carlo simulations are used to calculate the ground-state properties of the system with trial wave functions containing a parameter dependent on the amplitude and wavelength of the perturbation. The induced charge is most efficiently extracted from the difference in ground-state energies at different magnitudes of the external field, rather than directly from the expectation value of the density fluctuation operator. Results are compared to the random-phase approximation for the weakly coupled fluid and to classical lattice values at low densities where the system forms a Wigner crystal. The dielectric function is also calculated at intermediate fluid densities and the transition from positive to negative response is found to occur in the metallic regime.

INTRODUCTION

The dielectric function provides a compact description of electrical response properties such as screening, polarization, and plasma oscillations. The physical quantity of interest is actually the reciprocal $1/\epsilon(\mathbf{k},\omega)$, which gives the causal response to a perturbation. The dielectric function is defined in linear-response theory in terms of the ratio between the induced charge density and an external charge, which acts as a probe. The probe is assumed to be sufficiently weak so that the response is determined entirely by the properties of the unperturbed system. Furthermore, each Fourier component is treated as if it acts independently—a given potential $\phi(\mathbf{k},\omega)$ induces a density fluctuation of the same wave number $\mathbf{k}$ and frequency ω. The dielectric response may in principle be obtained by perturbation theory and the literature contains a number of models for the dielectric function, which approximately incorporate direct, exchange, and correlation contributions.

This paper is concerned with electrostatic ($\omega=0$) response at $T=0$. The dielectric function is obtained by perturbing the ground-state system with a sinusoidal external field $A_{\rm ext}\cos(\mathbf{q}\cdot\mathbf{r})$. The resulting induced charge density is calculated directly as the expectation value of the density-fluctuation operator and from the change in ground-state energy as a function of the amplitude of the applied field $A_{\rm ext}$. The quantum Monte Carlo method is particularly suited to the second approach, since it accurately calculates total energies from first principles. The algorithm has previously been applied to obtain ground-state properties of charged bosons[1], fermions,[1] and solids.[2,3]

The simplest system that can be used for a meaningful demonstration of this methodology for calculating the dielectric function is one consisting of charged bosons. Though not found except perhaps in astrophysical applications, the charged Bose gas is a useful model for superconducting systems and has an obvious relationship with the physically important fermion electron gas. Quantum Monte Carlo simulations of the boson ground state[1,4] have revealed three distinct physical regimes, defined in terms of the dimensionless measure of the density $r_s=r_0/a_0$ (where r_0 is related to the volume per particle by $\Omega/N=4\pi r_0^3/3$ and a_0 is the Bohr radius). The Bose gas is a weakly coupled fluid when $r_s\ll 1$. At lower densities, the system becomes a strongly coupled fluid and eventually undergoes a zero-temperature phase transition to form a Wigner crystal ($r_s>160$).

Previous calculations of the dielectric response of charged bosons have been based on several approximations. In the high-density limit, expressions for the dielectric function have been found to the next order to the Bogoliubov prescription[5] and in the random-phase approximation (RPA).[6] The perfect lattice response obtained from classical dynamics[7] has been used as a reasonable model of the Wigner crystal behavior at sufficiently low densities. The strongly coupled fluid is difficult to treat by perturbation theory due to the absence of any small expansion parameter. For metallic densities ($1\le r_s\le 10$), numerical solutions of the hypernetted-chain equations[8] have been used to obtain approximate values for the static linear-response function. The quantum Monte Carlo approach described here yields exact numerical values for the dielectric function within statistical error bars over the complete range of densities.

DIELECTRIC RESPONSE

Maxwell's equations define the macroscopic longitudinal response of charged systems in terms of the electric field $\mathbf{E}$, the displacement $\mathbf{D}$, and the external, induced, and total electrostatic potentials ϕ and charge densities ρ. Written in Fourier space,

$$\begin{aligned} i\mathbf{k}\cdot\mathbf{D}(\mathbf{k},\omega)&=-k^2\phi_{\rm ext}(\mathbf{k},\omega)=4\pi\rho_{\rm ext}(\mathbf{k},\omega)\ ,\\ i\mathbf{k}\cdot\mathbf{E}(\mathbf{k},\omega)&=-k^2\phi_{\rm total}(\mathbf{k},\omega)\\ &=4\pi\rho_{\rm total}(\mathbf{k},\omega)=4\pi[\rho_{\rm ext}(\mathbf{k},\omega)+\rho_{\rm ind}(\mathbf{k},\omega)]\ , \end{aligned} \tag{1}$$

and the reciprocal dielectric function is

$$\frac{1}{\epsilon(\mathbf{k},\omega)} \equiv \frac{\mathbf{E}(\mathbf{k},\omega)}{\mathbf{D}(\mathbf{k},\omega)} = \frac{\phi_{\text{total}}(\mathbf{k},\omega)}{\phi_{\text{ext}}(\mathbf{k},\omega)} = \frac{\rho_{\text{total}}(\mathbf{k},\omega)}{\rho_{\text{ext}}(\mathbf{k},\omega)} = 1 + \frac{\rho_{\text{ind}}(\mathbf{k},\omega)}{\rho_{\text{ext}}(\mathbf{k},\omega)} , \quad (2)$$

valid as long as the fields are small enough to neglect higher-order terms. With suitable quantum statistical definitions of the fields, potentials, and densities, the above equations also define the microscopic response for all $\mathbf{k}$ and ω.

In order to determine $\epsilon(\mathbf{k})$, the uniform background of a system of charge density $\rho_0(\mathbf{r}) = -ZeN/\Omega$ is sinusoidally deformed according to the prescription $\rho_0(\mathbf{r}) + \rho_{\text{ext}}(\mathbf{q})\cos(\mathbf{q}\cdot\mathbf{r})$, where N is the number of particles of charge Ze in the volume Ω. To first order this will induce a change in the charge distribution of the same form, $\rho_0(\mathbf{r}) + \rho_{\text{ind}}(\mathbf{q})\cos(\mathbf{q}\cdot\mathbf{r})$. The Hamiltonian can be written in terms of the external field or potential creating this deformation:

$$H = H_0 + H_{\text{ext}}, \quad H_0 = -\sum_{i=1}^{N} \frac{1}{r_s^2}\nabla_i^2 + \frac{2Z^2}{r_s}\sum_{i<j}^{N}\frac{1}{r_{ij}} ,$$
$$H_{\text{ext}} = A_{\text{ext}}\sum_{i=1}^{N}\cos(\mathbf{q}\cdot\mathbf{r}_i) = Ze\sum_{i=1}^{N}\phi_{\text{ext}}(\mathbf{r}_i) \quad (3)$$

(throughout this paper energies are in Ry and lengths are in $r_0 = r_s a_0$). The relation between the potential and external charge is given by the Poisson equation

$$\rho_{\text{ext}}(\mathbf{r}) = -\frac{\nabla^2\phi_{\text{ext}}(\mathbf{r})}{4\pi} = \frac{q^2}{4\pi}\phi_{\text{ext}}(\mathbf{r}) = \frac{q^2}{4\pi}\frac{A_{\text{ext}}}{Ze}\cos(\mathbf{q}\cdot\mathbf{r}) ,$$
$$\rho_{\text{ext}}(\mathbf{k}) = \frac{k^2}{4\pi}\frac{A_{\text{ext}}}{Ze}\frac{1}{(2\pi)^3}\int d^3r e^{-i\mathbf{k}\cdot\mathbf{r}}\left[\frac{e^{i\mathbf{q}\cdot\mathbf{r}} + e^{-i\mathbf{q}\cdot\mathbf{r}}}{2}\right]$$
$$= \frac{A_{\text{ext}}q^2}{8\pi Ze}[\delta_{\mathbf{k},\mathbf{q}} + \delta_{\mathbf{k},-\mathbf{q}}] . \quad (4)$$

The induced charge is the difference between the expectation value of the charge-density operator in the perturbed system $|\psi_A\rangle$ and in the original system $|\psi_0\rangle$

$$\rho_{\text{ind}}(\mathbf{k}) \equiv \langle\psi_A|\hat{\rho}_{\mathbf{k}}|\psi_A\rangle - \langle\psi_0|\hat{\rho}_{\mathbf{k}}|\psi_0\rangle$$
$$= \langle\hat{\rho}_{\mathbf{k}}\rangle_A - \langle\hat{\rho}_{\mathbf{k}}\rangle_0$$
$$= \frac{Ze}{\Omega}\left[\left\langle\sum_{i=1}^{N} e^{-i\mathbf{k}\cdot\mathbf{r}_i}\right\rangle_A - \left\langle\sum_{i=1}^{N} e^{-i\mathbf{k}\cdot\mathbf{r}_i}\right\rangle_0\right] . \quad (5)$$

In a homogeneous system, $\langle\hat{\rho}_{\mathbf{k}}\rangle_0 = 0$ as long as $\rho_{\text{ext}}(\mathbf{k}) = 0$ [and $\epsilon(\mathbf{k},\omega) \neq 0$], but this is not true in general. For the sinusoidal external field, ρ_{ind} is nonzero only for the wave vectors $\pm\mathbf{q}$ by the assumption of linearity

$$\rho_{\text{ind}}(\mathbf{k}) = [\langle\hat{\rho}_{\mathbf{k}}\rangle_A - \langle\hat{\rho}_{\mathbf{k}}\rangle_0][\delta_{\mathbf{k},\mathbf{q}} + \delta_{\mathbf{k},-\mathbf{q}}] .$$

Hence, according to the definition, the dielectric function is

$$\frac{1}{\epsilon(\mathbf{q})} = 1 + \frac{\rho_{\text{ind}}(\mathbf{q})}{\rho_{\text{ext}}(\mathbf{q})} = 1 + \frac{8\pi Ze}{A_{\text{ext}}q^2}[\langle\hat{\rho}_{\mathbf{q}}\rangle_A - \langle\hat{\rho}_{\mathbf{q}}\rangle_0]$$
$$= 1 + \frac{12Z^2}{A_{\text{ext}}Nr_s q^2}\left[\left\langle\sum_{i=1}^{N} e^{-i\mathbf{q}\cdot\mathbf{r}_i}\right\rangle_A - \left\langle\sum_{i=1}^{N} e^{-i\mathbf{q}\cdot\mathbf{r}_i}\right\rangle_0\right] . \quad (6)$$

The dielectric response can also be calculated from the change in ground-state energies at different amplitudes of the applied field. The derivative of the energy yields the induced density

$$\frac{dE(A_{\text{ext}})}{dA_{\text{ext}}} = \frac{d}{dA_{\text{ext}}}\langle\psi_A|H|\psi_A\rangle$$
$$= \left\langle\psi_A\left|\frac{\partial H}{\partial A_{\text{ext}}}\right|\psi_A\right\rangle = \frac{\Omega}{Ze}\langle\hat{\rho}_{\mathbf{q}}\rangle_A .$$

Expanding the induced charge for small A_{ext} and using the preceding equation to replace $\langle\hat{\rho}_{\mathbf{q}}\rangle_A$ in terms of the energy

$$\left[\langle\hat{\rho}_{\mathbf{q}}\rangle_A - \langle\hat{\rho}_{\mathbf{q}}\rangle_0\right] \approx A_{\text{ext}}\left.\frac{d\langle\hat{\rho}_{\mathbf{q}}\rangle_A}{dA_{\text{ext}}}\right|_{A_{\text{ext}}=0}$$
$$= \frac{Ze}{\Omega}A_{\text{ext}}\left.\frac{d^2E(A_{\text{ext}})}{dA_{\text{ext}}^2}\right|_{A_{\text{ext}}=0} ,$$

we obtain an alternative formula for the dielectric response

$$\frac{1}{\epsilon(\mathbf{q})} = 1 + \frac{8\pi(Ze)^2}{\Omega q^2}\left.\frac{d^2E(A_{\text{ext}})}{dA_{\text{ext}}^2}\right|_{A_{\text{ext}}=0}$$
$$= 1 + \frac{12Z^2}{Nr_s}\frac{1}{q^2}\left.\frac{d^2E(A_{\text{ext}})}{dA_{\text{ext}}^2}\right|_{A_{\text{ext}}=0} . \quad (7)$$

The value for the second energy derivative is obtained as twice the coefficient of the quadratic term in a polynomial fit to $E(A_{\text{ext}})$.

QUANTUM MONTE CARLO METHOD

For any Hamiltonian $\mathbf{H}$, the ground-state energy is the minimum of the expectation value with respect to all possible trial functions $\Psi_T(\mathbf{R})$

$$E_0 = \min_{\Psi_T(\mathbf{R})}\frac{\int\Psi_T(\mathbf{R})\mathbf{H}\Psi_T(\mathbf{R})d\mathbf{R}}{\int|\Psi_T(\mathbf{R})|^2 d\mathbf{R}} , \quad (8)$$

where the integration is over the $3N$ particle coordinates $\mathbf{R} = (\mathbf{r}_1, \mathbf{r}_2, \ldots, \mathbf{r}_N)$. In variational quantum Monte Carlo, the Metropolis method is used to evaluate the integrals numerically by sampling an ensemble of configurations $\mathbf{R}$ from the probability function

$$P(\mathbf{R}) = \frac{|\Psi_T(\mathbf{R})|^2}{\int|\Psi_T(\mathbf{R})|^2 d\mathbf{R}} .$$

The configurations are generated so that the random walk has an acceptance ratio of around 50%. The energy is given by the weighted sum

$$E_0 \leq \bar{E} = \sum_j P(\mathbf{R}_j) E_L(\mathbf{R}_j) ,$$

where $E_L = H\Psi_T(\mathbf{R})/\Psi_T(\mathbf{R})$ is the local energy and $\bar{E}$ is a strict upper bound for E_0 within statistical error bars. The form of $\Psi_T(\mathbf{R})$ is critical for convergence. The optimal choice is a trade off between computationally fast analytic functions and more accurate but complicated forms, which are slower to evaluate. Typically, the variational process is performed on a subset of trial functions with the minimization used to fix any free parameters.

The diffusion quantum Monte Carlo algorithm[9] solves the imaginary time many-body Schrödinger equation in the short time-step approximation. Examination of the formal asymptotic solution shows that the results converge exponentially fast to the ground state and yield a rigorous upper bound to the energy. The actual equation solved is the Schrödinger equation written in terms of the mixed distribution $f(\mathbf{R},\tau) = \Psi(\mathbf{R},\tau)\Psi_T(\mathbf{R})$,

$$-\frac{\partial f}{\partial \tau} = -\sum_{i=1}^{N} \frac{\hbar^2}{2m} [\nabla_i^2 f - \nabla_i \cdot (f \nabla_i \ln |\Psi_T|^2)] + (E_L(\mathbf{R}) - E_T) f , \tag{9}$$

where the trial energy E_T is a constant introduced for computational efficiency. Interpreting $f(\mathbf{R},\tau)$ as the density of configurations $\mathbf{R}$, the formal Green's-function solution

$$f(\mathbf{R}',t+\tau) = \int d\mathbf{R}\, G(\mathbf{R}\rightarrow\mathbf{R}',\tau) f(\mathbf{R},t), \quad f(\mathbf{R},0) = |\Psi_T(\mathbf{R})|^2$$

$$G(\mathbf{R}\rightarrow\mathbf{R}',\tau) = \left[\frac{4\pi\hbar^2}{2m}\right]^{-3N/2} \exp\left[-\frac{\left[\mathbf{R}'-\mathbf{R}-\frac{\tau\hbar^2}{2m}\nabla \ln|\Psi_T(\mathbf{R})|^2\right]^2}{\frac{4\tau\hbar^2}{2m}} \right] e^{\{-\tau[E_L(\mathbf{R})+E_L(\mathbf{R}')]/2+\tau E_T\}} . \tag{10}$$

corresponds to a diffusion process with directed drift and branching (birth and death) terms. Typically, configurations generated by the variational algorithm are taken as the starting point and new configurations are generated using time steps chosen to give an acceptance ratio in the 99th percentile. For bosons, spin statistics do not limit the convergence and the diffusion method is theoretically exact once time-step extrapolation to the $\tau\rightarrow 0$ limit is performed. However, a good trial function plays a critical role in importance sampling the diffusion process in order to obtain rapid convergence and good error bars.

In diffusion simulations, expectation values are calculated on the mixed distribution $\Psi_T\Psi$. Ψ_T affects only the variance and not the expectation value of the energy and $E_d \rightarrow E_0$. For other quantities, such as the density-fluctuation operator, the diffusion process generates mixed expectation values O_d, which lie between the variational O_v, and the exact results O_0. Linear extrapolation $O_0 \approx 2O_d - O_v$ can be used to obtain improved ground-state values.

For bulk systems, the Schrödinger equation is solved for a system of N particles in a periodic cell. The long-range Coulomb interactions are evaluated using Ewald sums which include the interactions between the simulation box particles and all of their periodic images. Extrapolation to the $N\rightarrow\infty$ limit is performed by simulating systems of increasing size to determine the number dependence.

The trial function used in the dielectric problem is a perturbation of the ground-state solution,[1] written schematically as

$$\Psi_T(\mathbf{R}) = e^{\sum_{i<j} u(r_{ij})} e^{\gamma \sum_i^N \cos(\mathbf{q}\cdot\mathbf{r}_i)} \prod_{i=1}^{N} \phi^B(\mathbf{r}_i) \approx e^{\sum_{i<j} u(r_{ij})} \left[1+\gamma \sum_i^N \cos(\mathbf{q}\cdot\mathbf{r}_i)\right] \prod_{i=1}^{n} \phi^B(\mathbf{r}_i) , \tag{11}$$

where the $\phi^B(\mathbf{r}_i)$ are single-particle orbitals. The $r_{ij} = |\mathbf{r}_i - \mathbf{r}_j|$ term is the Jastrow factor, which takes into account two-body correlations as well as the cusp condition for zero particle separation required by the singularity in the Coulomb potential. The single-particle boson orbitals are chosen to be the lowest-energy ($\mathbf{k}=0$) plane-wave states at fluid densities and Gaussian functions centered on the lattice sites for the crystal phase. The cosine term in Eq. (11) is the simplest form of the linear response to a sinusoidal external field of wave vector $\mathbf{q}$. It is written as an exponential to ensure that the wave function is everywhere positive. γ is a parameter that depends on the amplitude and wave vector of the applied field and may be found by variational minimization or solved for analytically in the RPA

$$\gamma^{\mathrm{RPA}} = \frac{-A_{\mathrm{ext}} r_s^2}{(q^4 + 12Z^2 r_s)^{1/2}} \tag{12}$$

(we omit the rather lengthy derivation).

RESULTS

In order to be consistent with periodic boundary conditions, an integer multiple of the applied field wavelength must exactly fit the simulation box. An additional constraint is that the charge variations not be too rapid for accurate sampling—the maximum number of wavelengths per box is typically no more than three for $N < 250$. The amplitudes of the applied fields are chosen as small as possible, consistent with obtaining statistically meaningful energy differences. Linear-response assumptions are then tested by checking that the expectation value of the density-fluctuation operator $\langle \rho_{\mathbf{k}} \rangle$ is zero within statistics for values of $\mathbf{k} \neq \pm\mathbf{q}$ and that the fits of energy versus amplitude show only quadratic behavior.

The most accurate and computationally efficient method of calculating the dielectric function is from Eq.

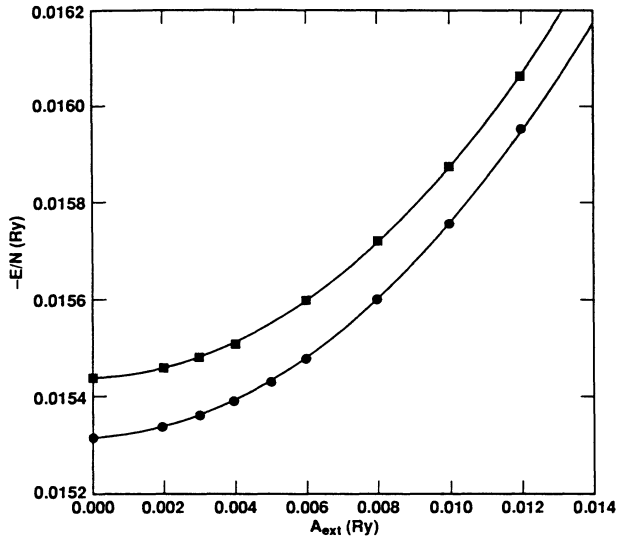

FIG. 1. Plot of variational (circles) and diffusion (squares) energies vs amplitude of the applied field at $r_s=100$, $N=64$, and $q=0.974\,44$. Error bars are smaller than the symbols. Energies are in Ry, and wave vectors in units of $1/r_0$. The curves are the quadratic fits.

(7), since the quantum Monte Carlo method yields exact ground-state energies. An example is shown in Fig. 1 for $r_s=100$, $N=64$, and $q=0.974\,44$. (Energies are in Ry, lengths in r_0, and wave vectors in $1/r_0$.) The solid lines are fits of the variational (circles) and diffusion (squares) points

$$-E^V(A_{\rm ext})/N=0.015\,321(1)+4.38(1)A_{\rm ext}^2\ ,$$

$$-E^D(A_{\rm ext})/N=0.015\,440(1)+4.36(1)A_{\rm ext}^2\ ,$$

with the error in the last digit given in parentheses. There is no evidence of higher-order contributions to the fits over this amplitude range. The variational and diffusion results agree within statistics (compare the coefficients of $A_{\rm ext}^2$), confirming that a reasonable choice for the trial wave function has been made. The error bars decrease as more field strengths are used in the fit, but typically dielectric values quoted in this paper were obtained using only the ground state and three amplitudes of the applied field.

The dielectric function can also be obtained from the expectation value of the charge density-fluctuation operator. Table I shows results for $r_s=10$ and $q=1.948\,89$ in the columns labeled ρ_q, with the superscripts indicating variational (V), diffusion (D), and extrapolated (X) values. The results are divided by appropriate constants to allow direct comparison to the second derivatives of the energy, which are also given in the table. All but one of the extrapolated values agree with the derivatives within statistics. However, to obtain converged values of $\langle\hat{\rho}_q\rangle_A$ of the same accuracy as the energies in general requires considerably longer simulations or an improved choice of the trial wave function. For average length runs, the charge fluctuation values for different amplitudes of the applied field typically do not agree within error bars and, at RPA densities, it is not possible to obtain statistically meaningful results. This reflects the difficulty in obtaining accurate mixed expectation values, exacerbated in this case since the weak perturbation is not strongly selected by the Monte Carlo procedure. A differential Monte Carlo scheme to obtain all field values simultaneously ran into related convergence problems, since the energy differences and differential weights require an accurate determination of $\langle\rho_q\rangle_A$.

The fluctuation dissipation formula

$$\frac{1}{\epsilon(q)}=1-\frac{4\pi e^2}{q^2\Omega}\int_0^\beta d\tau\langle T_\tau\rho(q,\tau)\rho(-q,0)\rangle \qquad (13)$$

TABLE I. Induced charge and second energy derivatives at $r_s=10$ and wavevector $q=1.948\,89$ for several amplitudes $A_{\rm ext}$, and different numbers of particles N in the simulation box. The energy derivatives quoted for each $A_{\rm ext}$ are obtained using all field amplitudes up to and including that value. The columns labeled ρ_q give the value of $\Omega\langle\hat{\rho}_q\rangle/ZeNA_{\rm ext}$, with the superscripts V, D, X indicating variational, diffusion, and extrapolated estimators, respectively. Errors in the last digit are indicated by the value in parentheses. Energies are in Ry.

N	$A_{\rm ext}$	$-\frac{E^V}{N}$	$-\frac{1}{N}\frac{d^2E^V}{dA_{\rm ext}}$	$-\rho_q^V$	$-\frac{E^D}{N}$	$-\frac{1}{N}\frac{d^2E^D}{dA_{\rm ext}^2}$	$-\rho_q^D$	$-\rho_q^X$
216	0.000	0.121 12(1)			0.121 469(5)			
	0.010	0.121 31(1)		3.25(3)	0.121 644(5)		3.48(3)	3.71(5)
	0.015	0.121 550(9)		3.26(2)	0.121 891(5)		3.52(2)	3.78(2)
	0.020	0.121 873(9)	3.75(6)	3.28(1)	0.122 220(6)	3.78(4)	3.50(1)	3.72(3)
	0.030	0.122 80(1)	3.72(3)	3.275(9)				
64	0.000	0.121 73(2)			0.122 073(9)			
	0.010	0.121 90(2)		3.21(5)	0.122 276(8)		3.51(4)	3.81(7)
	0.015	0.122 15(2)		3.30(3)	0.122 490(9)		3.57(3)	3.84(5)
	0.020	0.122 48(2)	3.8(1)	3.31(2)	0.122 841(8)	3.80(6)	3.48(2)	3.65(3)
8	0.000	0.127 59(2)			0.127 87(1)			
	0.010	0.127 79(2)		3.3(1)	0.128 07(1)		3.65(7)	4.0(1)
	0.015	0.128 03(2)		3.37(6)	0.128 33(1)		3.62(5)	3.87(9)
	0.020	0.128 30(2)	3.6(2)	3.28(5)	0.128 64(1)	3.88(8)	3.55(3)	3.82(7)

gives an expression for the dielectric function in terms of the density-density correlation function in imaginary time. However, in ground-state simulations, exact values for τ-dependent quantities cannot be obtained by straightforward extrapolation of mixed estimators and diffusion results do not provide a good approximation to the correlation function due to the convergence problem discussed in the preceding paragraph. Moreover, to reduce the error bars it is necessary to average the diffusion values over a range of τ, which smooths out the fluctuation behavior, making it difficult to extract the imaginary time dependence or accurately test consistency with an exponential decay form for the integrand.

Quantum Monte Carlo results for a given **q** must be extrapolated to the bulk limit using a set of simulations in which the number of wavelengths in the box is increased, matched by an increase in the number of particles. Table I shows the number dependence at $r_s=10$ and $q=1.948\,89$ for the three system sizes $N=8$, 64, and 216 corresponding to one, two, and three wavelengths in the simulation box, respectively. The values obtained from $N=8$ are generally least reliable as they show proportionally greater boundary effects. While the energies show significant number dependence, the dielectric response derived from the difference in ground-state energies is the same within statistics for the three systems (columns labeled $d^2E/dA_{\rm ext}^2$). This was similarly verified at the densities $r_s=1$ and 100 (see Table II), and confirmed by comparison of the finite N results with analytic values in the RPA limit and the Wigner crystal. Thus dielectric-function values can be obtained without explicitly performing the $N\rightarrow\infty$ extrapolation, a considerable time saving.

The diffusion Monte Carlo method also requires an extrapolation to remove the finite time-step approximation.

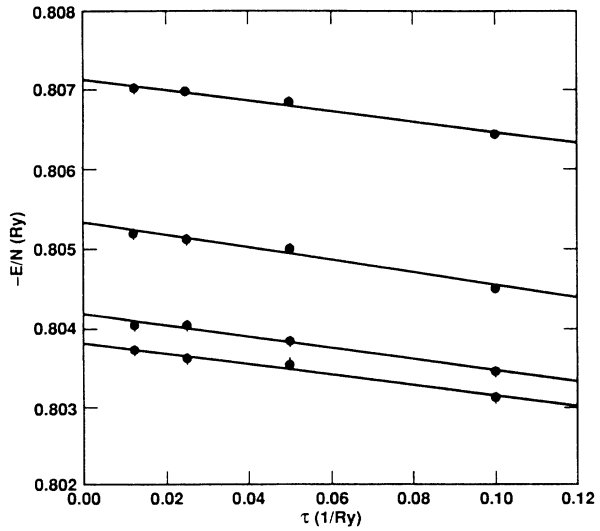

FIG. 2. Time-dependence plots of energy for $r_s=1$ and $N=64$ and applied wave vector $q=0.974\,44$. Error bars are shown by vertical lines and are on the order of the symbol size. The straight lines show the best linear fits for the four applied field amplitudes $A_{\rm ext}=0.0,0.1,0.2,0.3$ (from bottom to top).

Figure 2 shows a typical set of results at $r_s=1$. Energy is plotted versus the imaginary time step τ for the ground state and three amplitudes of the applied field. The data may be fitted to linear functions with the same slope, so the dielectric function obtained from the $\tau\rightarrow 0$ extrapolation is identical within error bars to that calculated directly from diffusion runs at any fixed but finite value of τ. Time-step dependence was checked explicitly at $r_s=1$, 10, and 100 (Table II) and implicitly at the two extreme densities by comparison with analytic results.

Dielectric-function values obtained via the energy

TABLE II. Inverse dielectric function from quadratic energy fits at five r_s values. The † indicates $\tau\rightarrow 0.0$ extrapolation and the * indicates values obtained from only one applied field amplitude. The superscripts V and D indicate variational and diffusion energy derivative values, respectively, while X labels extrapolated charge fluctuation results. The m indicates metastable systems. Errors in the last digit are indicated by the value in parentheses. Wave vectors are in units of $1/r_0$.

r_s	q	N	$\frac{1}{\epsilon^V}$	$\frac{1}{\epsilon^D}$	$\frac{1}{\epsilon^x}$
0.0025	0.974 44	[64]	0.968(3)	0.9681(6)	
	0.773 42	[128]	0.94(1)	0.925(6)*	
	0.613 80	[256]	0.80(6)*	0.84(2)*	
1.0	1.948 89	[216]	0.51(2)	0.500(3)	0.51(6)
		[64]	0.53(2)	0.505(3)	0.53(9)
		[8]	0.52(2)	0.503(4)	0.55(1)
	1.546 85	[16]	0.27(2)	0.271(7)	0.27(2)
	0.974 44	[64]	0.1(1)	0.07(2)	0.06(3)
		[64]		0.07(2)†	
	0.773 42	[128]	0.0(1)	0.02(2)	
10.0	1.948 89	[216]	−0.18(2)	−0.19(1)	−0.182(6)
		[64]	−0.20(3)	−0.20(2)	−0.19(1)
		[8]	−0.13(5)	−0.22(3)	−0.23(2)
	1.546 83	[16]	−0.140(7)	−0.141(4)	−0.125(5)
	0.974 44	[64]	−0.11(3)	−0.09(2)	−0.05(1)
	0.773 42	[128]	−0.07(4)	−0.06(2)	
	0.649 63	[216]	−0.03(5)	0.02(2)	
	0.487 22	[512]	−0.033(8)		
100.0	2.923 33	[64]	−1.75(4)	−2.20(3)	
	1.948 89	[64]	−0.54(2)	−0.57(2)	−0.56(1)
		[8]	−0.50(4)		
	1.546 83	[16]	−0.310(5)	−0.311(3)	
	1.031 22	[54]	−0.13(1)	−0.121(9)	
	0.974 44	[64]	−0.108(4)	−0.101(3)	
		[64]		−0.102(3)†	
	0.773 42	[128]	−0.037(3)	−0.06(2)	
	0.649 63	[216]	−0.04(1)	−0.04(3)	
100.0m	1.031 22	[54]	−0.079(7)	−0.119(8)	
100.0m	0.773 42	[128]	−0.024(9)	−0.02(1)	
200.0	3.093 67	[16]	−2.41(2)	−3.18(1)	
	2.062 45	[54]	−0.56(2)	−0.66(1)	
	1.546 85	[16]	−0.24(3)	−0.41(3)	
	1.031 22	[54]	−0.08(5)	−0.12(2)	
	0.773 42	[128]	−0.03(8)	−0.04(8)	
200.0m	1.031 22	[54]	−0.03(6)	−0.16(4)	
200.0m	0.773 42	[128]	−0.13(9)	−0.09(5)	

derivative approach are listed in Table II for several wave vectors at five different densities. Results for each q are from a single N value and from a fixed time step rather than $\tau \rightarrow 0$ extrapolated values in the case of diffusion, unless explicitly noted. Results for $\epsilon(\mathbf{q})$ obtained by direct evaluation of the density-fluctuation operator are given where converged and are useful both as a consistency check and for confirmation that we are operating in the linear regime. Cases for which the variational and diffusion results differ significantly must be treated with caution, since they indicate convergence problems and the breakdown of the importance sampling trial wave function. We first discuss the two extreme density regimes, where analytic results exist for comparison.

High-density weakly coupled fluid

In the weak-coupling regime $r_s \ll 1$ numerical difficulties require that the system be simulated by scaling the density r_s and charge Ze by factors of α according to the prescription

$$r_s^{\mathrm{SCALE}} = \alpha r_s, \quad (Z^{\mathrm{SCALE}})^2 = Z^2/\alpha \ .$$

The system of charge Z^{SCALE} at density r_s^{SCALE} and applied field $A_{\mathrm{ext}}^{\mathrm{SCALE}} = A_{\mathrm{ext}}/\alpha^2$ then gives the energies in units of $E^{\mathrm{SCALE}} = \alpha^2$ Ry for the corresponding system of charge Z and r_s and external field A_{ext}. To test the algorithm, we performed a few simulations at $r_s = 2.5 \times 10^{-3}$ ($\alpha = 400$). The trial function with γ^{RPA} is expected to be a very good approximation to the exact solution and, in fact, the variational and diffusion energies are identical within statistics. Results for the dielectric function are also in excellent agreement with the analytic expression derived by Hore and Frankel in the RPA limit (see Table III),[6]

$$\epsilon(\mathbf{q}, T=0) = 1 + \frac{4m_e^2\omega_p^2}{\hbar^2 q^4} = 1 + \frac{12 r_s}{q^4} \ ,$$

$$\text{where } \omega_p^2 = 4\pi N e^2/\Omega m_e = 3e^2/m_e r_0^3 \ , \quad (14)$$

shown by the solid curve in Fig. 3.

Low-density strong-coupling regime

For $r_s > 160$, the Bose gas forms a Wigner solid and the usual definition of the dielectric function does not apply due to the inhomogeneous nature of the crystal phase. The induced charge includes components at all wave vectors $\mathbf{q}+\mathbf{G}$, where $\mathbf{G}$ is a reciprocal lattice vector of the crystal. However, the directionally dependent macroscopic response, which neglects all fluctuations due to the reciprocal lattice vectors giving the induced charge only at the applied wave vector $\mathbf{q}$,[7,10] can be obtained using the external field method.

Table II and Fig. 4 show the results from quantum

TABLE III. Comparison of RPA dielectric function and quantum Monte Carlo results at $r_s = 0.0025$ for several wave vectors q. The superscripts V, D, RPA indicate variational, diffusion, and RPA values, respectively. The * indicates values obtained from a single applied field. Errors in the last digit are indicated by the value in parentheses. Energies are in Ry and lengths in r_0.

q	$\frac{1}{\epsilon^V}$	$\frac{1}{\epsilon^D}$	$\frac{1}{\epsilon^{\mathrm{RPA}}}$
0.974 44	0.968(3)	0.9681(6)	0.9678
0.773 42	0.94(1)	0.925(6)*	0.923
0.613 8	0.80(6)*	0.84(2)*	0.83

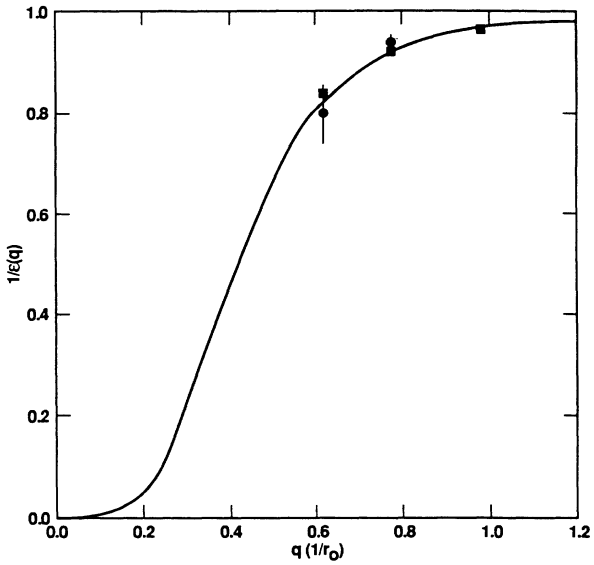

FIG. 3. Inverse dielectric function vs wave vector at $r_s = 0.0025$. The solid line shows the RPA solution of Hore and Frankel. Variational points are indicated by circles, diffusion values by squares, and error bars by vertical lines.

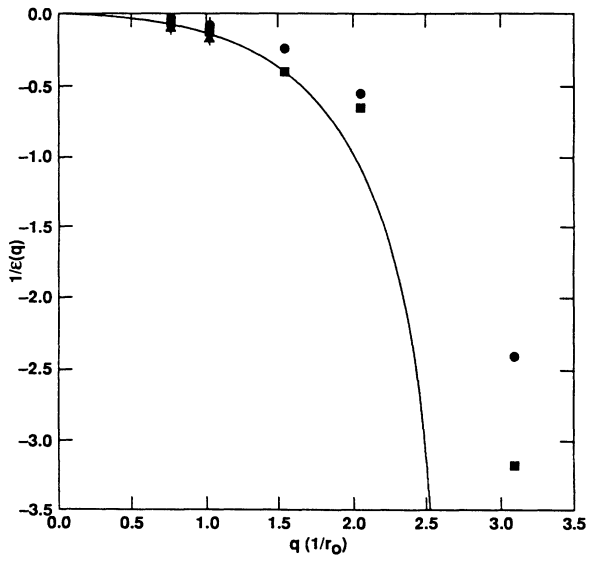

FIG. 4. Inverse dielectric function vs wave vector at $r_s = 200$. The solid line shows the classical lattice solution of Bagchi in the [100] direction. Variational points are indicated by circles, diffusion values by squares, and error bars by vertical lines. The triangles are the metastable diffusion values.

Monte Carlo calculations of the dielectric function at $r_s = 200$. The Wigner crystal is treated by explicitly binding the bosons to bcc lattice sites using Gaussians with a width parameter determined by variational minimization of the energy. The bosons are not very localized, the optimal width being on the order of the interparticle spacing. The difference between the variational and diffusion results is due in part to incomplete convergence of the variational runs and in part to the less optimal nature of the trial wave-function form at this density. We did not feel it worthwhile to carry out extensive number-dependence simulations, since localization reduces boundary effects. Comparison with the ideal lattice confirms that the quantum Monte Carlo results show no significant time-step or finite-size effects.

At such low densities, statistical contributions are expected to be small compared to Coulomb effects, so the classical system should provide a good starting point for examining boson (and fermion) ground-state properties. Using the harmonic approximation, Bagchi[7] derived the classical longitudinal macroscopic dielectric function of a crystal in the long-wavelength static limit

$$\epsilon(\mathbf{q}) \rightarrow 1 - \frac{\omega_p^2}{a^2 q^2}, \quad (aq)^2 \ll \omega_p^2 ,$$

where a is defined in terms of the small q dispersion relation

$$\omega_l^2 = \omega_p^2 - a^2 q^2 .$$

The bcc lattice dispersion relations have been calculated for specific directions in reciprocal lattice space by Coldwell-Horsfall and Maradudin.[11] Taking their value for a^2 for the [100] direction used in our simulations, we obtain the perfect lattice dielectric function valid for small q

$$\epsilon(\mathbf{q}) \rightarrow 1 - \frac{16\pi}{1.486} \left[\frac{3}{8\pi} \right]^{2/3} \frac{1}{q^2} . \tag{15}$$

To get an idea to what degree the Bose gas approximates the classical system, note that the static energy of the bcc lattice is $E_{\mathrm{bcc}} = -1.791\,86/r_s = -0.008\,959\,3$, while our ground-state energy values range from -0.0080 to -0.0081 Ry, depending on N. The 10% difference indicates that quantum effects will be small but not negligible. Bagchi's classical function is plotted as a solid curve in Fig. 4 and shows good agreement with our results for small q, particularly in the case of diffusion, confirming the dominance of localization effects. The quantum Monte Carlo values diverge from the curve for $q > 1.5$, not surprisingly, since the classical formula is valid only for $q \ll 2.8636$ by the criterion given above. From an examination of the sum rules for the classical lattice, Bagchi[7] concluded that ϵ should in fact be negative for all $\mathbf{q}$. At all wave vectors we examined for the quantum crystal, the induced charge is indeed of opposite sign from the external perturbation and becomes several times greater in magnitude as $\mathbf{q}$ approaches the charge-density wave vector associated with the Wigner crystal. The large discrepancy between the variational and diffusion values for such q indicates the breakdown of the chosen trial wave-function form, so the numerical values must be treated with some caution. For comparison, note that the classical lattice model exhibits the behavior $\epsilon \rightarrow 0, 1/\epsilon \rightarrow -\infty$ at reciprocal lattice wave vectors (i.e., $q = 3.093\,67$ in the [100] direction).

Strongly coupled fluid

We performed simulations in the intermediate density regime $1 \leq r_s \leq 160$ to study the transition from weak to strong coupling. Quantum Monte Carlo results are given for three densities in Table II: $r_s = 1$ (metallic fluid), $r_s = 10$ (low-density fluid), and $r_s = 100$ (partially localized fluid), where the physical classification is based on an examination of the pair correlation functions $g(r)$ shown in Fig. 5. The trial function used in the simulations was the perturbed fluid form with the parameter γ determined by the RPA solution and checked by variational minimization. Time-step and number-dependence checks were explicitly carried out at all three densities.

Figure 6 plots results obtained at $r_s = 1$. The values show a high degree of correspondence with the RPA solution of Hore and Frankel (solid line), despite the fact that interactions can no longer be considered negligible. This is not completely unexpected, however, since it has been noted that the condensate fraction of the Bose gas remains close to one even at $r_s = 2$, so that Bogoliubov (and RPA) theory is not a bad approximation for typical metallic densities.[4]

The dielectric function at $r_s = 10$ is plotted in Fig. 7. Comparison with Fig. 6 shows that a qualitative change in dielectric behavior from positive to negative response has occurred. In fact, the quantum Monte Carlo results

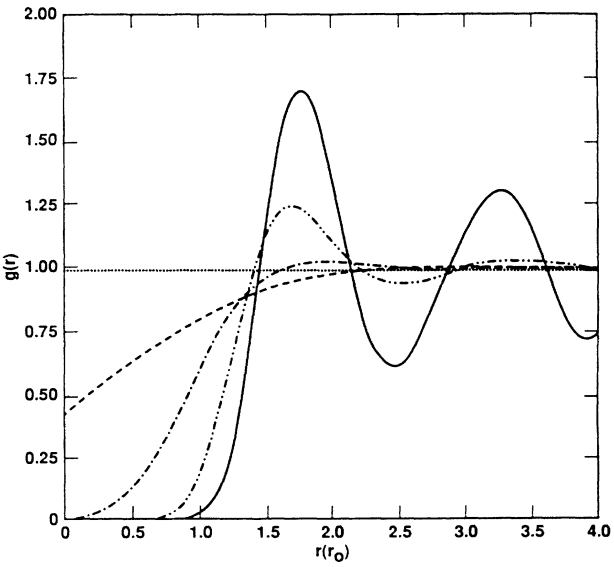

FIG. 5. Pair-correlation function for $N = 128$ at the five r_s densities for which dielectric functions were obtained. The dotted line is $r_s = 0.0025$, the dashed line is $r_s = 1$, the dot-dashed line is $r_s = 10$, the double-dotted-dashed line is $r_s = 100$, and the solid line is $r_s = 200$. Note that the length scales are different for the five curves.

correspond with the classical Bagchi prediction for the [100] direction at longer wavelengths (plotted as the solid line) even though the fluid does not exhibit much localization—the pair-correlation function in Fig. 5 has a hole near $r=0$, but only the barest trace of the peaks characteristic of the crystal.

Although early workers argued from stability considerations that ϵ must always be positive, the Kramers-Kronig relations show that the actual restriction on the inverse dielectric function[10,12] is $[1/\epsilon(\mathbf{q})] \leq 1$, which does not preclude the existence of negative static dielectric values at nonzero q. For the fermion electron gas, the change in sign of the response occurs at $r_s \approx 5$ and is associated with a change in sign of the compressibility. This transition density is much higher than that at which the system becomes unstable with respect to the (charge-density wave) crystal state. Our results indicate that for bosons, negative response also appears somewhere in the metallic regime ($1 < r_s < 10$). However, examination of the Bose equation of state[4] shows that this transition is not related to a change in sign of the compressibility.

The $r_s = 100$ values are plotted along with the classical dielectric curve in Fig. 8. The fluid at this density exhibits considerable localization, with strong peaks at distances related to the lattice spacing of the Wigner crystal (compare the $r_s = 100$ and 200 curves in Fig. 5). Despite the fact that we are using fluid trial functions, the dielectric response is basically indistinguishable from the Wigner crystal case as can be seen by superimposing the curves, recalling that lengths are scaled by r_0. In fact, the crystallization transition is not sharply marked for the bosons as reflected by the small binding energy of the solid.

As a check, we calculated the dielectric function of the metastable fluid at $r_s = 200$ and the metastable crystal at $r_s = 100$. The values obtained are listed in Table II, with the diffusion results plotted as triangles in Figs. 4 and 8. Within statistical accuracy it is not possible to distinguish between the localized and delocalized states at either of the two densities.

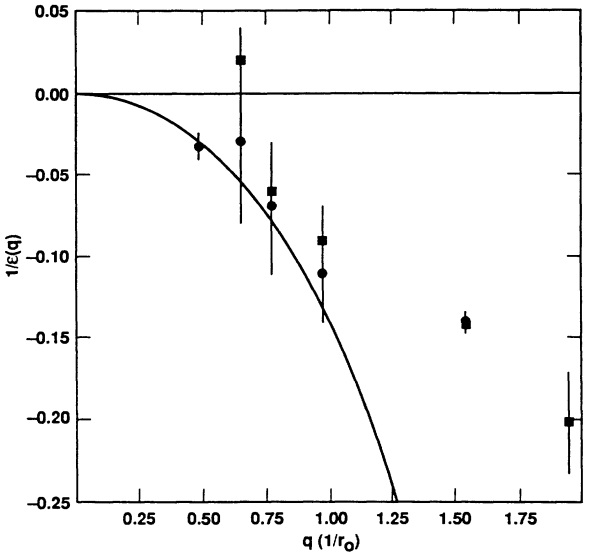

FIG. 7. Inverse dielectric function vs wave vector at $r_s = 10$. The solid line shows the classical lattice solution in the [100] crystal direction. Variational points are indicated by circles, diffusion values by squares, and error bars by vertical lines.

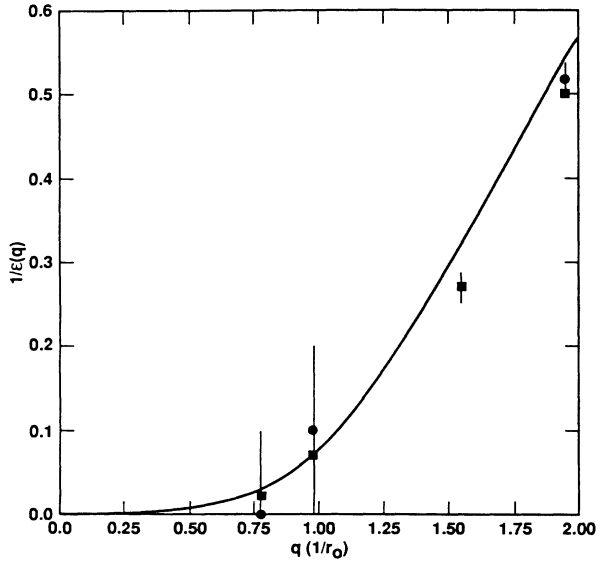

FIG. 6. Inverse dielectric function vs wave vector at $r_s = 1$. The solid line shows the RPA solution. Variational points are indicated by circles, diffusion values by squares, and error bars by vertical lines when they are larger than the symbols.

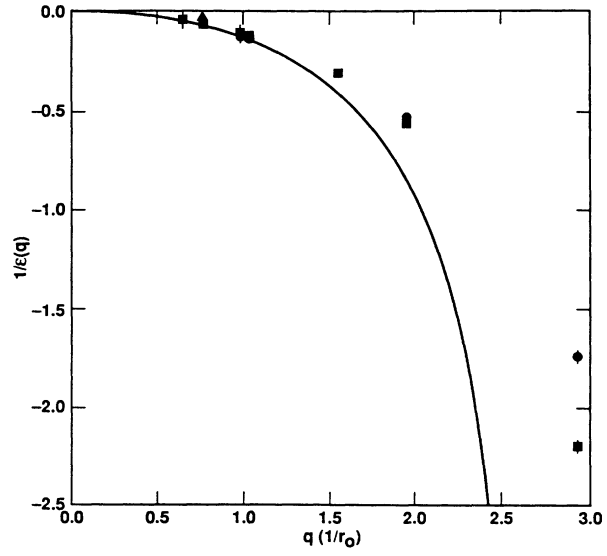

FIG. 8. Inverse dielectric function vs wave vector at $r_s = 100$. The solid line shows the classical lattice solution in the [100] crystal direction. Variational points are indicated by circles, diffusion values by squares, and error bars by vertical lines when they are larger than the symbols. Triangles are the metastable diffusion values.

In summary, we have performed calculations of the dielectric function of the charged Bose gas over the entire range of interesting densities. The algorithm is currently being extended to treat the fermion electron gas. The primary difficulties to be resolved concern the form of the perturbed trial function, extrapolation to the bulk limit, and improvement of the statistical accuracy of the results.

ACKNOWLEDGMENTS

The authors wish to thank D. Ceperley, who originally interested us in this project, and R. Pollock and K. Runge for useful discussions. This work was performed under the auspices of the U.S. Department of Energy Lawrence Livermore National Laboratory Contract No. W-7405-ENG-48.

---

*Also at Department of Applied Science, University of California, Davis, CA 95616.

[1]D. Ceperley and B. J. Alder, Phys. Rev. Lett. **45**, 566 (1980).

[2]D. Ceperley and B. J. Alder, Phys. Rev. B **36**, 2092 (1987).

[3]G. Sugiyama, G. Zerah, and B. J. Alder, Physica A **156**, 144 (1989); D. M. Ceperley and B. J. Alder, Phys. Rev. B **36**, 2092 (1987).

[4]J.-P. Hansen and R. Mazighi, Phys. Rev. A **18**, 1282 (1978), and references cited therein.

[5]J. Lee, Phys. Rev. B **12**, 2644 (1975).

[6]S. Hore and N. Frankel, Phys. Rev. B **12**, 2619 (1975).

[7]A. Bagchi, Phys. Rev. **178**, 707 (1969), and references cited therein.

[8]M. Saarela, Phys. Rev. B **28**, 191 (1984).

[9]P. Reynolds, D. Ceperley, B. J. Alder, and W. Lester, J. Chem. Phys. **77**, 5593 (1982).

[10]O. V. Dolgov, D. A. Kirzhnits, and E. G. Maksimov, Rev. Mod. Phys. **53**, 81 (1981); O. V. Dolgov and E. G. Maksimov, Usp. Fiz. Nauk. **138**, 95 (1982) [Sov. Phys. Usp. **25**, 688 (1982)]; D. A. Kirzhnits and A. A. Maradudin, in *The Dielectric Function of Condensed Systems*, edited by L. V. Keldysh (North-Holland, Amsterdam, 1989).

[11]R. A. Coldwell-Horsfall and A. A. Maradudin, J. Math. Phys. **1**, 395 (1960).

[12]P. Allen, M. Cohen, and D. Penn, Phys. Rev. **B38**, 2513 (1988).